ROMANIAN JOURNAL OF INFORMATION SCIENCE AND TECHNOLOGY
Volume **13**, Number 4, 2010, 358–367

Two-Steps Profile Diffractive Microlenses Design to Generate Binary Focal Points Along The Propagation Axis

Mona MIHĂILESCU[1], Arcadie SOBETKII[2], Mihaela PELTEACU[3]

[1] *Politehnica* University of Bucharest
313 Splaiul Independenţei, Bucharest, Romania
E-mail: mona_m@physics.pub.ro

[2] SC OPTICOAT SRL
5 Răcari Str., Bucharest, Romania
E-mail: arcadie@opticoat.ro

[3] SC OPTOELECTRONICA SRL
409 Atomiştilor Str., Măgurele, Romania
E-mail: mihaela@optoel.ro

Abstract. The aim of our study is to find a simple design for the two-steps profile diffractive micro-lenses (DMLs) which will generate binary focal points on the propagation axis at monochromatic plane wave incidence. Their fabrication steps include e-beam lithography (for mask pattern) and reactive ion etching (for transparent DMLs). For the two-steps profile, the fabrication process is simpler because it doesn't introduce errors due to masks alignment. In the design algorithm, developed in MATLAB, we start with simple DMLs which generate one single focal point at a given distance. We propose a method which uses some sections from different simple DMLs to built one DML with special properties. We investigate the influence of the missing zones in the diffraction pattern. The propagation was simulated in the Fresnel approximation. To visualize their transparent binary microrelief and the phase profile, we employ the digital holographic microscopy technique. Experimental and simulation results are presented.

Key words: Diffractive microlenses, Fresnel approximation, digital holographic microscopy.

1. Introduction

Diffractive microlenses (DMLs) have several advantages besides the refractive ones and the main one consists in their micro-relief of the order of hundreds of nanometers. Considering this feature, they are incorporated in different devices leading to the achievement of lower weights and lengths of the whole system. The diffractive micro-lenses are important for parallel laser writing systems, pickup head, ophthalmic applications [1, 2, 3]. The profile of these DMLs can be binary or continuous, with advantages and disadvantages for each of them, set off in a comparative study [4]. Using a proper design, they have the ability to create simultaneously two focal points situated along the propagation axis.

In this paper we present our design to obtain diffractive micro-lenses which generate two focal points along the optical axis. The simple superposition of two diffractive micro-lenses with different focal distances generates multiple parasite peaks in diffractive pattern besides the useful ones. Our idea was to combine sections from two Fresnel zone plates (FZPs) with different geometrical and optical parameters.

In the second part, we describe the technological processes to fabricate these DMLs and the digital holographic microscopy technique to visualize and measure the phase difference introduced by them, which is the start point for depth profile measurements.

The criterion to compare different DMLs has been chosen in the behavior of the intensity values behaviour along the propagation axis, experimentally or simulated using the Fresnel approximation.

2. Wavefield propagation

We consider a monochromatic, unit amplitude plane wave of the wavelength λ, normally incident on a DML with the transmittance function $t(x, y)$ situated at $z = 0$, in the input plane. The complex diffracted field $U(x_z, y_z, z)$ at the distance z from the microlens, can be expressed using the 2-D convolution operator [5]:

$$U(x_z, y_z, z) = t(x, y, 0) \otimes h(x, y, x_z, y_z, z), \tag{1}$$

where

$$h(x, y, x_z, y_z, z) = \frac{\exp(ikr_{01})}{i\lambda r_{01}} \tag{2}$$

is the impulse response, x, y are the coordinates in the input plane, the DML plane, x_z, y_z are the coordinates in the output plane, the diffraction pattern plane (or the image plane), $k = 2\pi/\lambda$ and r_{01} is the distance between any two points from the input plane to the output plane.

In the Fresnel approximation, the impulse response from Eq. (1) has been written in a proper form for convolution operator and the complex amplitude of the diffracted field is given by:

$$U(x_z, y_z, z) = \frac{\exp(ikz)}{i\lambda z} \exp\left\{\frac{ik}{2z}\left[x_z^2 + y_z^2\right]\right\} \cdot$$

$$\cdot \int_{-\infty}^{\infty}\int_{-\infty}^{\infty} U'(x, y, 0) \exp\left[-i2\pi(xu + yv)\right] dxdy = O_{Fre}\left(t(x, y, 0)\right), \tag{3}$$

where

$$U'(x, y, 0) = t(x, y, 0) \exp\left\{\frac{ik}{2z}\left[x^2 + y^2\right]\right\}, \tag{4}$$

and $O_{Fre}\left(t(x, y, 0)\right)$ express the Fresnel transform operator, which is applied to the transmission function and changes the variables $(x,\ y)$ into the spatial frequencies

$$u = x_z/\lambda z, v = y_z/\lambda z. \tag{5}$$

For the numerical calculation, we sampled these functions at Nyquist frequency, taking care on the under-sampling, and implementing Eqs. (3) and (4) in discrete form using 2-D matrices and the Fast Fourier Transform (FFT) routines in MATLAB. The simulations were performed using the built-in MATLAB functions with the discrete variables (m, n), (m_z, n_z) given by:

$$x = m \cdot \Delta p, \quad y = n \cdot \Delta p, \quad x_z = m_z \cdot \Delta p_z, \quad y_z = n_z \cdot \Delta p_z, \tag{6}$$

where Δp and Δp_z are the pixels dimensions in the DML plane and in the image plane respectively. The link between them is given in [6]. By denoting with M the total number of pixels in both x and x_z directions, and with N the total number of pixels in y and y_z directions ($M = 1024$, $N = 1024$), then $m = \overline{1, M}$ and $n = \overline{1, N}$. Our implementation of the Fresnel approximation in MATLAB is largely described elsewhere [7].

The transmittance function $t(x, y)$ is also used in its discrete form and corresponds to the phase masks of the diffractive microlenses. They become in MATLAB, different $M{\times}N$ matrices with the phase values 0 and π for a binary profile.

We began with Fresnel zone plates generation, characterized by their own geometrical parameters (its number of zones, a, and the radius of each of them, r_a) in a relation with optical parameters (the focal distance f and the wavelength λ) given by [8]:

$$r_a^2 = 2fa\lambda. \tag{7}$$

An example is in Fig. 1a, where the focal length is 40 mm, $\lambda = 632.8$ nm and the number of the zones is $a = 67$.

The evolution of the axial intensity along the propagation axis z given by FZP is calculated using the above equations. The intensity values on the propagation axis given after diffraction on the FZP shown in Fig. 1a, are collected and plotted in Fig. 1b. To obtain two focal points on the propagation axis, it is necessary to combine some FZPs with different parameters. These simple FZPs have only two depth levels (black and white in Fig. 1a, 2a and 2b).

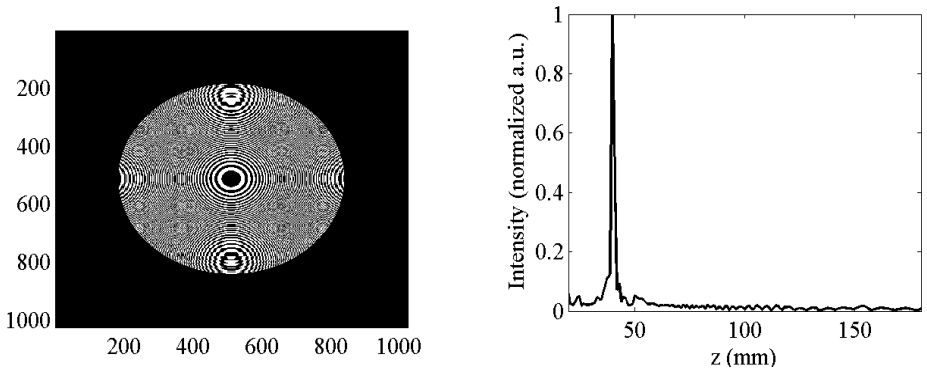

a) **b)**

Fig. 1. a) FZP generated for a focal distance of 40 mm; **b)** intensity values on the propagation axis.

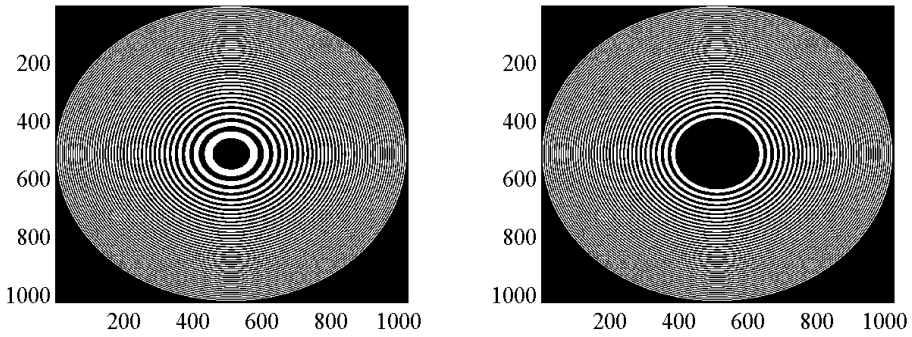

a) **b)**

Fig. 2. Diffractive microlenses calculated for a focal distance 152 mm: **a)** integral; **b)** 3 central zones missing.

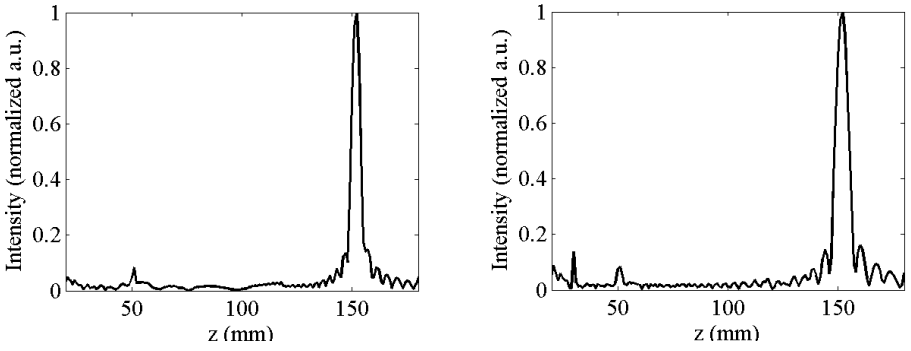

a) **b)**

Fig. 3. Intensity along propagation axis calculated for FZPs with focal distance 152 mm: **a)** integral; **b)** 17 central zones missing.

In Fig. 2a is a FZP calculated for a focal distance of 152 mm with all zones, and in Fig. 2b is the same FZP but with three missing central zones. In Fig. 3 are plotted the intensity values on the optical axis at different distances z, corresponding with FZPs designed like in Fig. 2. We noticed that the number of the zones influences the width of the focal peak. When all zones are present, the focalization is stronger.

3. Design

Using two simple DMLs, designed after Fresnel zone plates like is described in the previous section, we begin with the superposition of their microrelief. In this case, two possibilities were investigated: the rigorous one with four-steps profile (see Fig. 4a where are black and white levels, and also two gray levels) or the approximation with two steps profile (see Fig. 4b where are only black and white levels). The simulations performed in the same conditions like in the previous section, exhibit several unwanted peaks (see Fig. 4c and 4d). In the case of the DML designed like in Fig. 4a, the intensity behavior along propagation axis exhibits a greater signal to noise ratio (61%) besides the case of the DML designed like in Fig. 4b (28%), but the fabrication process includes two masks.

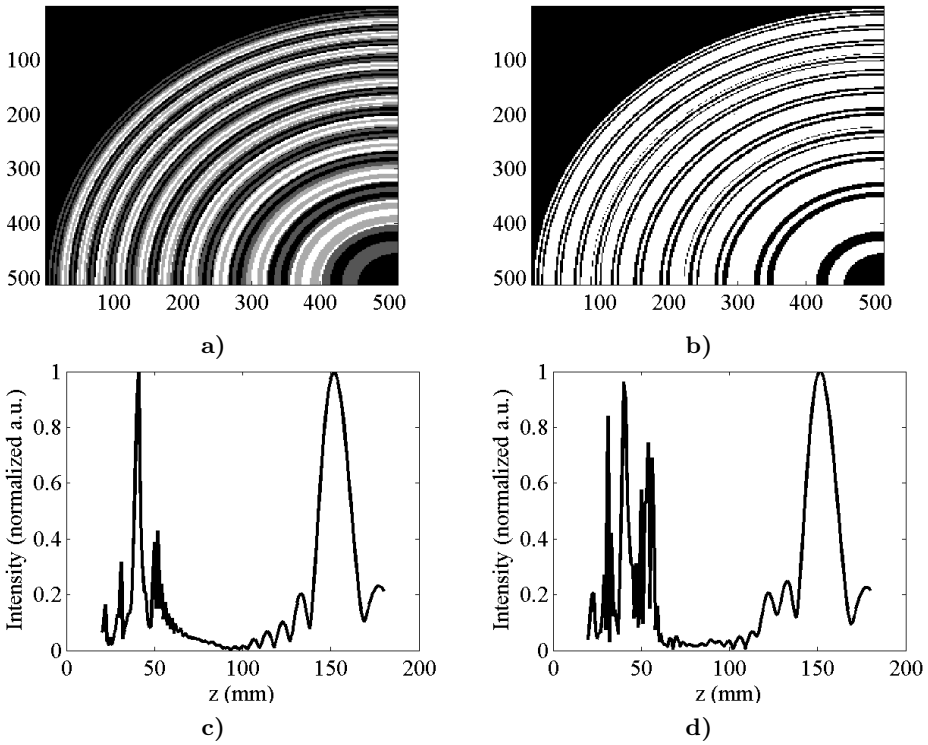

Fig. 4. The superposed DMLs obtained starting with the simple ones designed like in Fig. 1a and 2a with **a)** 4 levels: **b)** 2 levels; **c)** and **d)** the diffracted intensity along propagation axis with unwanted peaks from the DMLs designed like in Fig. 4a and b respectively.

To obtain two focal points on the optical axis, we combine different geometries of Fresnel zone plates. In Figs. 5 and 6 are shown two DMLs obtained starting with the FZP with the focal point situated at $z = 40$ mm and the FZP with the focal point situated at $z = 152$ mm, but in Fig. 5, 16 central zones are missing and in Fig. 6, 17 central zones are missing from the FZP with the focal point situated at $z = 152$ mm.

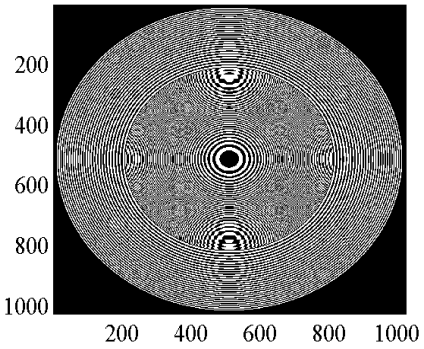

Fig. 5. The DML obtained after the combination of one FZP with the focal length 40 mm and one FZP with the focal length 152 mm and 16 missing central zones.

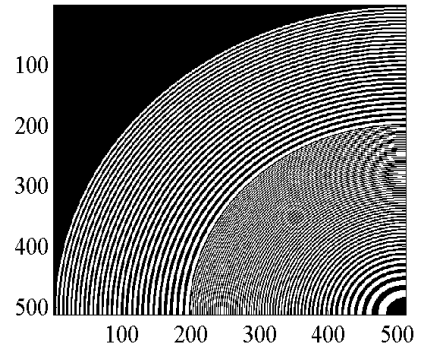

Fig. 6. A quarter from the DML obtained after the combination of: (1) one FZP with focal length 40 mm and (2) one FZP with focal length 152 mm and 17 missing central zones.

4. Fabrication and characterization

To fabricate the micro-lenses, two wafers are necessary: W1 from borosilicate glass on which will be produced the masks by e-beam lithography and W2 in which will be fabricated the DMLs. W2 plate consists of 2.54 mm thick polished borosilicate

glass, covered with thin film Cr+CrO_2 and 400–600 nm photoresist layer deposited by spinning at 1500 rpm and dried at 80°C at IR radiation. The mask pattern from W1 is recorded on W2 using UV radiation. The photoresist from W2 is developed and removed in the exposed area, followed by the chemical removal of Cr+CrO_2 after mask pattern, reactive ion etching of the glass from W2 where it is not covered by Cr+CrO_2 (different time intervals for different profile depths) and total chemical removal of the photoresist and Cr+CrO_2.

After the MATLAB design of the DMLs to produce two focal points on the propagation axis, we followed the above steps to fabricate DMLs with different pixel size and microrelief depth to find optimum values for different cases.

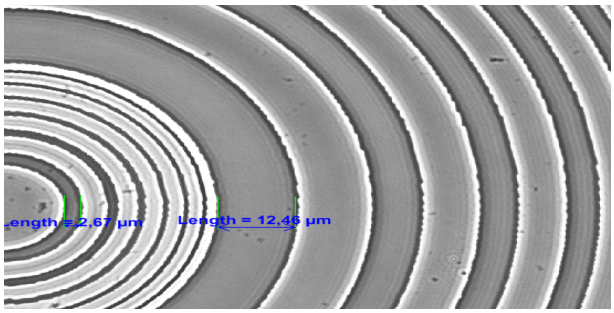

a)

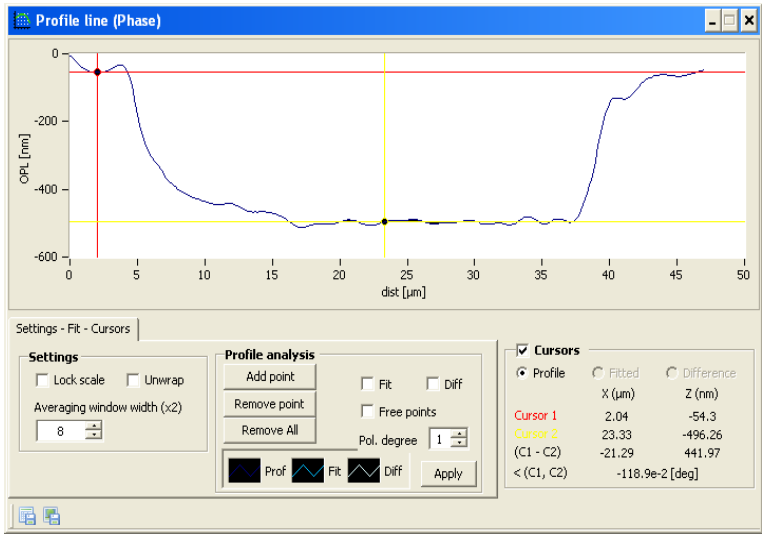

b)

Fig. 7. a) Phase contrast image of one DML; **b)** depth profile obtained using digital holographic microscopy (a part from the other DML).

The results for two of them are presented here with phase contrast microscopy (see Fig. 7a where only dimensions in xOy plane are available) and with digital holographic

microscopy (DHM). In the experimental setup for DHM, the transparent DML is arranged in the object arm and the interference pattern with the reference beam is recorded on the CCD. To obtain the 3D image of the object, a reconstruction process is performed using a dedicated software Koala. From this 3D image, the profile of the object allows depth measurements (see Fig. 7b). An advantage of this technique is that we can find the depth of the microrelief from the phase shift introduced by the sample, in the hypothesis that the object has a known refractive index (in our case 1.54 for borosilicate glass). The DHM technique is used in other laboratories to study blood cells, vibrating micromirrors, tumors inhomogeneity, microstructures, live organisms.

5. Results

The masks patterns from Figs. 5 and 6 (integral), generated in MATLAB, became phase only transmission function used as input data for Fresnel operator (Eq. 4). For both of them, intensity values obtained on the propagation axis are collected and plotted in Figs. 8 and 9, for the simulation case.

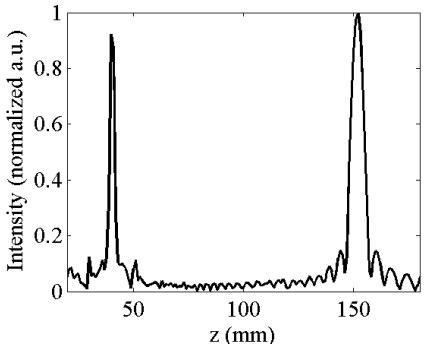

Fig. 8. Intensity values on the optical axis – simulated diffraction pattern given by the DML from Fig. 5.

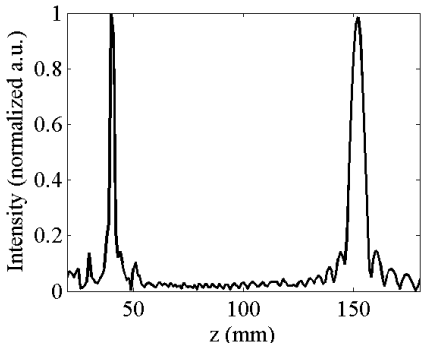

Fig. 9. Values on the optical axis from the simulated diffraction pattern given by the DML from Fig. 6.

One can easily observe that the number of the missed central zones is critical, not only in the width of the peaks, but also in the relative maximum intensity values of the peaks in the focal zones. In the first case, the peak from 40 mm is smaller than the peak from 152 mm (0.92 besides 1) and in the second case, the peaks have similar maximum values (1 besides 0.99).

We recorded on the CCD the diffracted intensity in these two focal planes and the images are shown in Fig. 10a at $z = 40$ mm and in Fig. 10b at $z = 152$ mm, when the phase mask is the fabricated one, after the design from Fig. 6. The experimental results are in agreement with the simulated ones with large focal point at $z = 152$ mm.

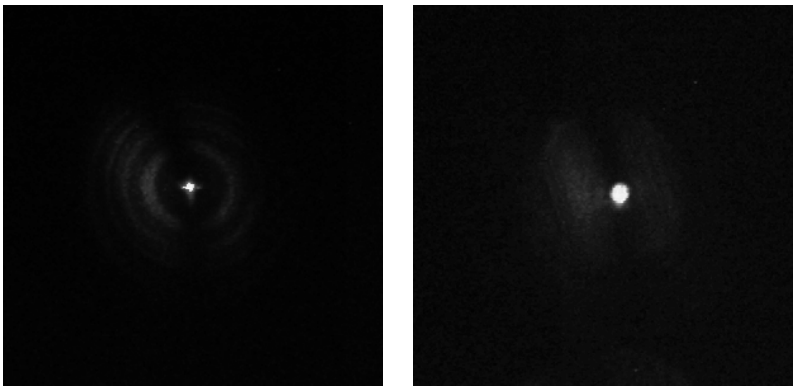

a) **b)**

Fig. 10. Experimentally diffracted intensity obtained from the DML from Fig. 6 (entire) recorded at **a)** $z = 40$ mm and **b)** $z = 152$ mm.

6. Conclusions

The superposition of two simple diffractive micro-lenses gives unwanted peaks in the intensity behaviour along propagation axis, even in the case of the four-steps DML. An unique combination of simple diffractive micro-lenses with different focal points, is proposed in this paper to design DMLs which generate two focal points along propagation axis. The influence of some missing zones is investigated and an increasing value for the width of the focal peak was noticed. The Fresnel approximation was used to simulate the diffracted field at different distances along propagation axis and these results are in agreement with experimental ones.

The designed DMLs after a combination of two Fresnel zone plates were fabricated using several steps including e-beam lithography (for mask) and reactive ion etching (for transparent DML in glass). When a monochromatic plane wave is incident on them, two focal points are obtained on the optical axis, in accordance with the simulation results. The phase profile of the fabricated DML was checked using digital holographic microscopy and the depth values were found for each reactive ion etching time interval for a given refractive index of the borosilicate glass.

Acknowledgements. The experiments were carried out using equipments acquired by contract #4/CP/I/2007 PNCDI II "Capacities", and the research has been (partially) supported by the ANCS-UEFISCSU grant #836-ID 1556/2009.

References

[1] Jiubin Tan, Mingguang Shan, Chenguang Zhao, Jian Liu, *Design and fabrication of diffractive microlens arrays with continuous relief for parallel laser direct writing*, Appl. Opt., vol. **47**, no. 5, pp. 1430–1433, 2008.

[2] Hui-Hsiung Lin, Mao-Hong Lu*, Synthesis of arbitrarily discrete, diffractionless beams using dual-wavelength diffractive objective lens for optical pickup head*, Opt. Express, vol. **18**, no. 3, pp. 2534–2548, 2010.

[3] Davison J. A., Simpson M. J., *History and development of the apodized diffractive intraocular lens*, J. Cataract Refract. Surg., vol. **32**, no. 5, pp. 849–858, 2006.

[4] Castignoles F., Flury M., Lepine T., *Comparison of the efficiency, MTF and chromatic properties of four diffractive bifocal intraocular lens designs*, Opt. Express, vol. **18**, no. 5, pp. 5245–5256, 2010.

[5] Goodman J. W., *Introduction to Fourier Optics*, Mc Graw-Hill Book Company, 1968.

[6] Garcia J., Mas D., Dorsch R. G., *Fractional-Fourier-transform calculation through the fast-Fourier-transform algorithm*, Appl. Opt., vol. **35**, no. 3, pp. 7013–7018, 1996.

[7] Mihailescu M., *Natural quasy-periodic binary structure with focusing property in near field diffraction pattern*, Opt. Express, vol. **18**, no. 12, pp. 12526–12536, 2010.

[8] O'Shea D. C., Suleski T. J., Kathman A. D., Prather D. W., *Diffractive Optics*, SPIE Press, Bellingham, Washington, USA, 2004.